Charge Equilibration Time of Slow, Highly Charged Ions in Solids

M. Hattass,[1,2] T. Schenkel,[1] A. V. Hamza,[1] A. V. Barnes,[1] M. W. Newman,[1,3] J. W. McDonald,[1]
T. R. Niedermayr,[1,4] G. A. Machicoane,[1,4] and D. H. Schneider[1]
[1]*Physics & Space Technology Directorate, Lawrence Livermore National Laboratory, University of California, Livermore, California 94550*
[2]*Institut für Kernphysik, J. W. Goethe Universität, 60486 Frankfurt am Main, Germany*
[3]*University of Connecticut, Department of Physics, Storrs, Connecticut 06269*
[4]*Laboratoire de Physique Atomique et Nucléaire, Universitée Pierre et Marie Curie, 75005 Paris, France*
(Received 9 December 1998)

We report observations of nonequilibrium charge state distributions of slow, highly charged ($33+ \leq q \leq 75+$) ions after transmission of thin carbon foils. Charge equilibration times are determined directly from the dependencies of exit charge states on projectile velocity ($0.5 \times 10^6 < v < 10^6$ m/s) and foil thickness (5–10 nm). Ions like Xe^{44+} and Au^{68+} are found to equilibrate inside of solid matter in a time of only 7 fs. [S0031-9007(99)09368-0]

PACS numbers: 34.50.Dy, 34.80.Lx, 78.90.+t

The interaction of slow ($v < 0.5 v_0$, $v_0 = 2.19 \times 10^6$ m/s = Bohr velocity), highly charged ions (SHCI) with solid surfaces is an active field of basic and applied physics [1,2]. Recent fundamental studies [3,4] have stimulated interest in the application of SHCI to challenges in surface characterization [5] and materials modification [6] on a nanometer length scale. It is a defining characteristic of SHCI like Xe^{44+} and Th^{75+} that their charge states are far in excess of the mean equilibrium charge states that ions develop inside of solids. The latter are $\sim 1+$ for velocities well below v_0 [4,7]. Potential energies of SHCI, i.e., the sum of binding energies of electrons that were removed when forming the ion, can be hundreds of keV (e.g., 198 keV for Th^{75+}). In the interaction with solids, this potential energy is deposited into small (nanometer scale) target volumes, creating conditions of intense, ultrafast electronic excitations. Knowledge of charge equilibration times of SHCI inside of solids is important for the understanding of microscopic deexcitation processes. In this Letter we report on the first observations of nonequilibrium charge state distributions of SHCI after interaction with a solid and determine the time required for charge equilibration of Xe^{44+} and Au^{68+} in carbon foils.

In the interaction of SHCI with solids, neutralization above surfaces has been described in a "classical over-the-barrier" model [1]. Here, resonant transfer of target electrons into Rydberg states results in formation of "hollow atoms"—highly excited projectiles with most of the initially present inner shell vacancies still empty. Auger and radiative transition rates are, however, too slow for relaxation into the ground state above the surface. When penetrating the solid, electrons in Rydberg states are "peeled off" and a more compact cloud of target electrons screens the highly excited projectile, i.e., a second hollow atom is formed below the surface [1,2]. The time scale for screening depends on electron capture cross sections for the given projectile-target combination and on the response of the target's electronic system [8]. Inside the solid, deexcitation proceeds via Auger and radiative transitions [1,2,9–11]. So far, SHCI have always been found to be fully equilibrated after passage through solid matter [4,12]. An upper limit for the charge equilibration time of Th^{65+} at $0.3 v_0$ in carbon was found to be 21 fs [4]. Deexcitation times <10 fs were indicated by preequilibrium energy loss enhancements for SHCI with $q > 40+$ [13]. However, direct measurements of charge equilibration times for SHCI inside of solids have so far not been available.

The experimental setup has previously been described [2,4]. SHCI (Xe^{33+} to Th^{75+}) were extracted from the electron beam ion trap at Lawrence Livermore National Laboratory. Targets were amorphous carbon foils mounted on high transmission grids [14]. We determined the thickness of target foils *in situ* through measurements of proton energy loss and comparison with literature data [15]. Values for foil thicknesses were 5 (± 0.6) and 10 (± 0.7) nm, or 1 (± 0.12) and 2 (± 0.14) $\mu\mathrm{g/cm}^2$. The residual gas pressure in the target region was kept below 10^{-8} Torr. After foil transmission, projectiles in different charge states were separated in the electric field of two parallel plates and detected by a position sensitive microchannel plate detector (PSD). The distance to the PSD was 130 cm. The detector had a solid angle of 2.5 msr and could be moved in the direction of charge separation. We did not observe significant variations in detection efficiency as a function of detector position. The beam flux was typically $\sim 10^3$ ions/s, and the total dose for any target was $< 10^9$ ions. Repeated measurements under identical conditions did not show any foil modifications. We calculated charge state populations and mean charge states, q_{ave}, by the normalization of counts in a given charge state distribution to the number of ion extraction cycles for which the spectrum was accumulated. Typical statistical errors for the q_{ave} were $\leq 10\%$.

In Fig. 1 we show charge state distributions for Au^{68+} after transmission of 5 and 10 nm thick carbon foils. The impact velocity was $0.45v_0$. We observe a shift towards higher exit charge states for the 5 nm ($q_{\mathrm{ave}} = 7.3+$) as compared to the 10 nm thick foil ($q_{\mathrm{ave}} = 2.0+$). The equilibrium charge state for gold ions at this velocity is about 1.9+ [7]. Almost complete charge equilibration is accomplished in the 10 nm foil, during a time of 10 fs. On the contrary, the time of 5 fs that ions spend in the 5 nm foil is clearly too short for complete deexcitation. The highest q_{ave} observed in this study was 8.2+ for Th^{75+} ions at $0.43v_0$ after transmission of a 5 nm foil (with $q_{\mathrm{ave}} = 2.9+$ for the 10 nm foil).

Transmitted projectiles were detected after flight times of a few μs, long enough for the decay of any surviving inner shell vacancies. Fluorescent yields for gold M-shell vacancies are $\sim$0.1 [16], and most vacancies decay through Auger transitions. In an estimated upper limit, the projectile charge state increases by +3 in the course of cascading processes outside the solid [17] following the filling of each surviving M-shell vacancy. Electronic configurations of transmitted projectiles were not probed directly in our experiment. However, charge state distributions in Fig. 1 are consistent with the presence of, on the average, less than one M-shell vacancy after transmission of the 10 nm foil, while for the 5 nm foil on average 2 of the initial 17 M-shell vacancies of Au^{68+} survive.

The dependency of q_{ave} on the initial charge state, q, is shown in Fig. 2 for Xe^{q+} and Au^{q+} at a constant velocity of $0.38v_0$. A value of $q_{\mathrm{ave}} = 2.5+$ had been determined for Xe^{1+} at the same velocity after the passage of 50 nm thick carbon foils [18]. For $\mathrm{Xe}^{33,44,50+}$ transmitting the 10 nm thick foil we found $q_{\mathrm{ave}} = 1.8+$ ($\pm$0.2). When the same ions passed through the 5 nm foil q_{ave} increased from 2.5+ ($\pm$0.3) to 4.6+ ($\pm$0.5). For Au^{68+} $q_{\mathrm{ave}}(10\ \mathrm{nm}) = 1.3+$ ($\pm$0.2), and $q_{\mathrm{ave}}(5\ \mathrm{nm}) = 5.3+$ ($\pm$0.5). At the given impact velocity of 8.3×10^5 m/s, ions spend about 6 fs inside the 5 nm thick foil. Loss of kinetic energy in the foil reduces the ion velocity by less than 4% [13].

Figure 3 shows the effect of projectile velocity ($0.23v_0 \le v \le 0.43v_0$) on q_{ave} for Xe^{44+}. The dotted line gives a comparison to mean equilibrium charge states q_{eq} that were calculated using Bohr's stripping criterion ($q_{\mathrm{eq}} = Z_{\mathrm{ion}}{}^{1/3} \times v/v_0$) [7]. Values for q_{ave} show only a weak increase for the 10 nm thick foil. However, the q_{ave} for the 5 nm foil increase significantly, indicating incomplete charge equilibration once the time spent inside the foil is decreased below about 7 fs.

An approach to describe the development of ion charge states in solids has to consider pertinent atomic collision parameters and the response of the target's electronic system to the perturbation by an SHCI [1,17,19]. A rigorous treatment would have to include nonlinear screening and would require knowledge of cross sections for multiple electron capture processes. Since none of the above is well known at this time, we assume that deexcitation of hollow atoms in a solid follows an exponential decay from the initial configuration with a charge state q_i to the equilibrium charge state q_{eq} [20]. The relaxation into charge state equilibrium is then given by

$$q(x) = q_{\mathrm{eq}} + (q_i - q_{\mathrm{eq}})e^{-\alpha(x/v)}. \qquad (1)$$

Here, x is the depth coordinate and α is an equilibration rate comprised of contributions from the formation of the screening cloud and a mean deexcitation rate which is averaged over all atomic transitions in the course of hollow atom relaxation. q_{eq} was calculated for each velocity from Bohr's stripping criterion. From a least square fit of our data for Xe^{44+} and Au^{68+} to this

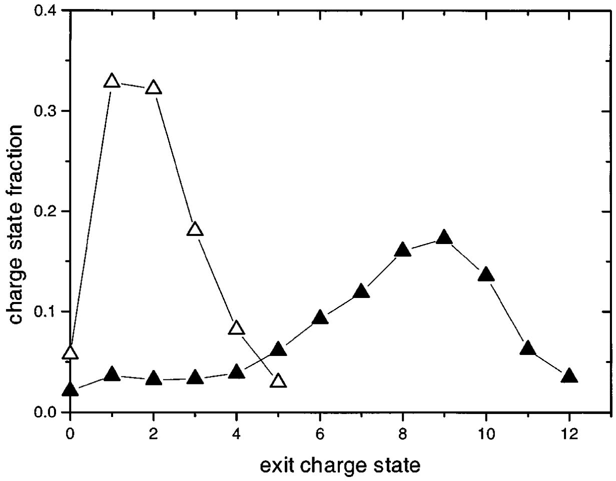

FIG. 1. Charge state distribution for Au^{68+} after transmission of thin carbon foils. The initial velocity was $0.43v_0$. Solid symbols, 5 nm thick foil; open symbols, 10 nm thick foil. Lines are shown to guide the eye.

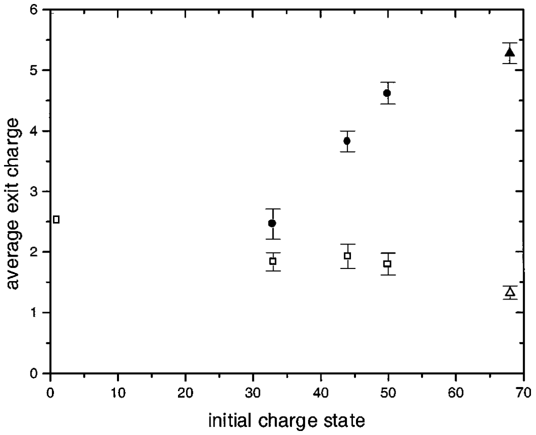

FIG. 2. q_{ave} for Xe^{q+} after transmission of carbon foils vs initial charge state. Open squares, 10 nm foil; solid circles, 5 nm foil. q_{ave} for Au^{68+}: open triangle, 10 nm foil; solid triangle, 5 nm foil. Data point for Xe^{1+} from [18]. The impact velocity was $0.38v_0$.

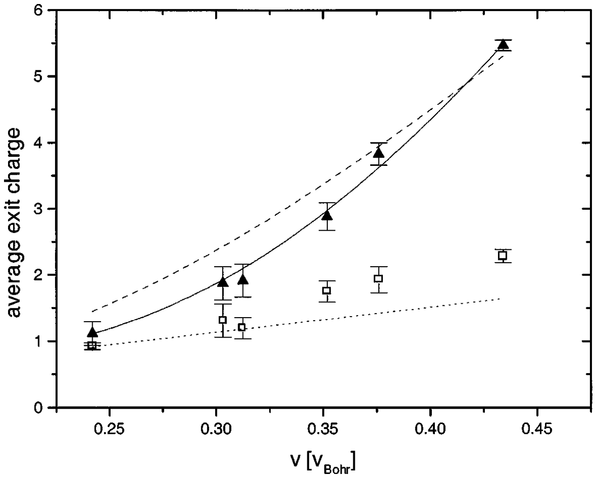

FIG. 3. q_{ave} of Xe^{44+} ions after transmission of foils vs initial projectile velocity. Open symbols, 10 nm foil; solid symbols, 5 nm foil. Dotted line: Bohr criterion; dashed line: Eq. (1); solid line: Eq. (3).

formula (Fig. 3, dashed line; Au^{68+} data not shown) we obtain $\alpha = 4.7 \times 10^{14}\ \text{s}^{-1}$ and $\alpha = 5.2 \times 10^{14}\ \text{s}^{-1}$, respectively.

The fit obtained from Eq. (1) describes the general trend of data in Fig. 3. In the following we attempt to improve the agreement in separating the influence of screening cloud formation and atomic transition rates. In this scenario, screening is not complete immediately after a projectile enters the solid, but requires a finite built-up time. During this time, the rate with which inner shell vacancies are filled is limited by the number of electrons in the screening cloud. Once the population of screening electrons saturates, the number of inner shell vacancies decays exponentially.

We express this in the following first order linear differential equation:

$$\frac{dq}{dt} = -\gamma(1 - e^{-\lambda t})q\,. \tag{2}$$

Here, λ is the rate with which the dynamic screening cloud is formed and γ is a mean deexcitation rate averaged over all atomic transitions in the course of charge equilibration. With boundary conditions $q(t = 0) = q_i$ and $q(t = \infty) = q_{\text{eq}}$ and setting $t = x/v$ we obtain now

$$q(x) = q_{\text{eq}} + (q_i - q_{\text{eq}})e^{-\gamma(x/v)}e^{-(\gamma/\lambda)(e^{-\lambda(x/v)}-1)}. \tag{3}$$

Fitting our data to this formula (Fig. 3, solid line) we obtain $\lambda = 4.3 \times 10^{14}\ \text{s}^{-1}$ with $\gamma = 7.6 \times 10^{14}\ \text{s}^{-1}$ for Xe^{44+} and $\gamma = 8.2 \times 10^{14}\ \text{s}^{-1}$ for Au^{68+}. The fit is significantly improved when separating the influence of screening and atomic transition rates.

Our analysis indicates that screening of the SHCI is incomplete during the first 2 fs after entering the solid. In the asymmetric combination of heavy projectiles incident on a light target, M-shell vacancies in Xe^{44+} and Au^{68+} cannot be filled directly [2,9,11]. Projectile levels with energies that allow for direct filling by carbon L-shell and (in close collisions) K-shell electrons have principal quantum numbers $n \geq 5$ for Au^{68+} ($n \geq 4$ for Xe^{44+}). At the velocities used in this study, SHCI travel 1 to 2 nm into the target during formation of the dynamic screening cloud. For Au^{68+}, screening at this rate requires capture of about ten electrons per atomic layer. Electrons in the screening cloud are both in bound and continuum states. The concept of an incompletely screened projectile for a time of a few fs is consistent with preequilibrium energy loss enhancements, and knowledge of charge equilibration times can contribute significantly to the understanding of microscopic energy loss mechanisms in the preequilibrium regime [13,21,22].

Deexcitation proceeds continuously while an SHCI is crossing a target surface. Assuming capture of carbon electrons into the lowest energetically allowed level, i.e., $n = 5$–6 for Au^{q+}, we can estimate a lower limit for the number of Auger transitions necessary to reach charge state equilibrium. For Au^{68+}, at least $\sim$100 transitions have to take place within 7 fs. Once the dynamic screening cloud is formed after a few fs, the number of inner shell vacancies in the hollow atom decays exponentially with a rate $\gamma = 8.2 \times 10^{14}\ \text{s}^{-1}$, and ten to twenty vacancies are filled during each of the first four intervals of $1/\gamma$. Typical transition rates for the filling of inner shell vacancies in hollow atoms are $\sim 10^{15}$ to $10^{16}\ \text{s}^{-1}$ [1,10,11]. Sequential filling of vacancies with these rates would take much longer than the observed equilibration times. We conclude that multiple transition cascades have to proceed in parallel to facilitate the rapid charge equilibration of SHCI.

Our study probes heavy SHCI incident on a light target material. Charge equilibration is expected to be faster when level matching [1] allows the direct filling of inner shell vacancies by target electrons. The rate of screening cloud formation is sensitive to electronic properties of target materials such as the concentration of conduction band electrons. The amorphous carbon used here is a semimetallic conductor. Screening times and, consequently, also charge equilibration times are expected to be even shorter for metals but significantly longer for insulators [21].

In summary, we have measured charge states of slow, highly charged ions after transmission of thin carbon foils. The time required to reach charge state equilibrium in a solid is determined to be only $\sim$7 fs for Xe^{44+} and Au^{68+}. Multiple Auger-transition cascades have to proceed in parallel to facilitate this rapid equilibration.

M. H. would like to thank Professor H. Schmidt-Böcking for his continuous support. This work was performed under the auspices of the U.S. Department of Energy by Lawrence Livermore National Laboratory under Contract No. W-7405-ENG-48.

[1] A. Arnau *et al.*, Surf. Sci. Rep. **27**, 113 (1997), and references therein.
[2] D. Schneider and M. A. Briere, Phys. Scr. **53**, 228 (1996), and references therein.
[3] T. Schenkel *et al.*, Phys. Rev. Lett. **81**, 2593 (1998); **80**, 4325 (1998); M. Sporn *et al.*, Phys. Rev. Lett. **79**, 945 (1997); T. Sekioka *et al.*, Nucl. Instrum. Methods Phys. Res., Sect. B **146**, 172 (1998).
[4] T. Schenkel *et al.*, Phys. Rev. Lett. **78**, 2481 (1997); Mater. Sci. Forum **248&249**, 413 (1997).
[5] T. Schenkel *et al.*, J. Vac. Sci. Technol. A **16**, 1384 (1998); A. V. Hamza *et al.*, *ibid.* **17**, 303 (1999).
[6] T. Schenkel *et al.*, J. Vac. Sci. Technol. B **16**, 3298 (1998); J. D. Gillaspy *et al.*, *ibid.* **16**, 3294 (1998); K. Suzuki and N. Itabashi, Pure Appl. Chem. **68**, 1011 (1996).
[7] N. Bohr, K. Dan. Vidensk. Selsk. Mat. Fys. Medd. **18**, 8 (1948); K. Shima *et al.*, Phys. Rev. A **40**, 3557 (1989).
[8] D. Pines, in *Solid State Physics*, edited by F. Seitz and D. Turnbull (Academic, New York, 1955), Vol. 1; U. Falke, Fresenius J. Anal. Chem. **349**, 241 (1994).
[9] R. Schuch *et al.*, Phys. Rev. Lett. **70**, 1073 (1993).
[10] R. Díez Muiño *et al.*, Phys. Rev. Lett. **76**, 4636 (1996).
[11] J. P. Briand *et al.*, Phys. Rev. A **53**, 2194 (1996); K. R. Karim *et al.*, J. Phys. B **29**, 4007 (1996).
[12] S. Winicki *et al.*, Phys. Rev. A **56**, 538 (1997); L. Folkerts *et al.*, Phys. Rev. Lett. **74**, 2204 (1995); A. Bürgi *et al.*, J. Appl. Phys. **73**, 4130 (1993).
[13] T. Schenkel *et al.*, Phys. Rev. Lett. **79**, 2030 (1997); Phys. Rev. A **56**, R1701 (1997).
[14] The carbon foils were provided by The Arizona Carbon Foil Co., Tucson, Arizona.
[15] R. Golser *et al.*, Nucl. Instrum. Methods Phys. Res., Sect. B **67**, 69 (1992).
[16] W. Bambynek *et al.*, Rev. Mod. Phys. **44**, 716 (1972).
[17] T. J. Gray *et al.*, Phys. Rev. A **16**, 1907 (1977), and references therein.
[18] R. Loew, Nucl. Instrum. Methods **118**, 505 (1974).
[19] B. Rosner *et al.*, Phys. Rev. A **57**, 2737 (1998).
[20] W. Brandt *et al.*, Phys. Rev. Lett. **30**, 358 (1973).
[21] M. A. Briere *et al.*, Phys. Scr. **T73**, 324 (1997).
[22] J. I. Juaristi *et al.*, Phys. Rev. Lett. **82**, 1048 (1999).